

First-principles results of electromagnetic properties for sd shell nuclei

Archana Saxena and Praveen C. Srivastava

Department of Physics, Indian Institute of Technology Roorkee, Roorkee 247 667, India

(Dated: December 14, 2024)

In this work we present *ab initio* shell-model calculations of electric quadrupole moments and magnetic dipole moments of sd shell nuclei using valence-space Hamiltonians derived with two *ab initio* approaches: the in-medium similarity renormalization group (IM-SRG) and the coupled-cluster effective interaction (CCEI). Results are in good agreement with the available experimental data as well as with results from the phenomenological USDB effective interaction. This work will add more information to available *ab initio* results for the spectroscopy of sd shell nuclei.

PACS numbers: 21.60.Cs, 21.30.Fe, 21.10.-k, 23.20.-g, 21.10.Ky, 27.20.+n, 27.30.+t

I. INTRODUCTION

The study of atomic nuclei using first principles is an important topic in nuclear structure physics. The anomalous behavior for nuclei close to the drip-lines can now be explained using *ab initio* approaches. The inclusion of three-body forces was found to be crucial for explaining the exact location of the drip-line for oxygen and calcium isotopes [1, 2]. Although *ab initio* calculations are difficult for heavier nuclei, recently spectroscopy of sd shell nuclei using different *ab initio* approaches has been reported in the literature. Using the in-medium similarity renormalization group (IM-SRG) approach, *ab initio* predictions for ground and excited states of doubly open-shell sd nuclei have been reported [3]. Also *ab initio* coupled-cluster effective interaction (CCEI) was derived and used to calculate levels in p and sd shell nuclei successfully [4–6]. A mass-dependent effective Hamiltonian in a $0\hbar\Omega$ model space for the sd shell nuclei, starting from a no core shell model Hamiltonian in a $4\hbar\Omega$ model space with the realistic JISP16 and chiral N3LO NN interactions has been reported in ref. [7]. The recent experimental results of ^{24}F have been theoretically interpreted with IM-SRG in ref. [8] and a coupled-cluster interpretation has been presented for recently populated levels in ^{25}F [9]. In all these papers, the focus was on the spectroscopy of p and sd shell nuclei.

In the present work, our motivation is to test the *ab initio* Hamiltonians derived from two approaches, IM-SRG and CCEI, by calculating electromagnetic properties of sd shell nuclei. The results of this work will add to the earlier studies in refs. [3–5, 7], where only spectroscopic properties (spins, parities and level energies) of these nuclei were reported. We compare our results to available experimental data as well as to calculations using the phenomenological USDB shell-model interaction [10].

The paper is organized as follows. In section II, we present details about the Hamiltonians from *ab initio* approaches. In section III, we present theoretical results along with experimental data wherever these are available. Finally, a summary and conclusions are presented in section IV.

II. HAMILTONIAN

In this work we performed shell model calculations for which the valence-space Hamiltonian was derived using two modern *ab initio* approaches: in-medium similarity renormalization (IM-SRG) [3] and coupled-cluster effective interaction (CCEI) [4]. We have also compared the results with calculations using the phenomenological USDB effective interaction [10]. For the diagonalization of the matrices we used the shell-model code NuShellX [11].

Using in-medium similarity renormalization group (IM-SRG) [12] based on chiral two- and three-nucleon interactions, Stroberg *et al.*, derived mass-dependent Hamiltonians for sd shell nuclei [3].

The starting Hamiltonian H that is normal ordered with respect to $|\Phi_0\rangle$

$$H = E_0 + \sum_{ij} f_{ij} \{a_i^\dagger a_j\} + \frac{1}{2!} \sum_{ijkl} \Gamma_{ijkl} \{a_i^\dagger a_j^\dagger a_l a_k\} + \frac{1}{3!} \sum_{ijklmn} W_{ijklmn} \{a_i^\dagger a_j^\dagger a_k^\dagger a_n a_m a_l\}, \quad (1)$$

where the normal ordered strings of creation and annihilation operators obey $\langle \Phi_0 | \{a_i^\dagger \dots a_j\} | \Phi_0 \rangle = 0$. The normal-ordered 0-, 1-, 2- and 3-body terms are E_0 , f_{ij} , Γ_{ijkl} and W_{ijklmn} , respectively (see ref. [13] for further details). Here, a continuous unitary transformation, parametrized by the flow parameter s , is applied to the initial normal-ordered A-body Hamiltonian.

$$H(s) = U^\dagger(s)H(0)U(s) = H^d(s) + H^{od}(s). \quad (2)$$

Where, $H^d(s)$ is the diagonal part of the Hamiltonian and $H^{od}(s)$ is the off diagonal part of the Hamiltonian. The evolution of $H(s)$ with s is given by

$$\frac{dH(s)}{ds} = [\eta(s), H(s)] \quad (3)$$

Where, $\eta(s)$ is the anti-Hermitian generator of unitary transformation

$$\eta(s) = \frac{dU(s)}{ds} U^\dagger(s) = -\eta^\dagger(s). \quad (4)$$

The off-diagonal matrix elements become zero as $s \rightarrow \infty$ for an appropriate value of $\eta(s)$. Here, the sd valence space is decoupled from the core and higher shells as $s \rightarrow \infty$. Now we use this resulting Hamiltonian in the shell model calculations with $\hbar\Omega = 24\text{MeV}$. Further details about the parameters are given in ref. [3].

There is another *ab initio* approach, named coupled cluster effective interaction, which we use in this paper for calculating the electromagnetic properties of nuclei in the sd shell. The effective interaction developed from this approach has already been successfully used to calculate the spectroscopy for open sd shell deformed nuclei [4]. For the effective interaction from this approach, we have also used a Hamiltonian which is A- dependent

$$\hat{H}_A = \sum_{i < j} \left(\frac{(\mathbf{p}_i - \mathbf{p}_j)^2}{2mA} + \hat{V}_{NN}^{(i,j)} \right) + \sum_{i < j < k} \hat{V}_{3N}^{(i,j,k)}. \quad (5)$$

The NN and NNN parts are taken from a next-to-next-to leading order (N2LO) chiral nucleon-nucleon interaction and a next-to-next-to-next-to leading order (N3LO) chiral three-body interaction, respectively. A cutoff scale $\Lambda = 500$ MeV is used for the NN part and $\Lambda = 400$ MeV for the NNN part. These interactions are constructed using the similarity transformation group method (see ref. [5] for further details). In this approach, a Hartree-Fock ground state in thirteen oscillator major shells with $\hbar\Omega = 20\text{MeV}$ is used. The CCEI Hamiltonian for shell model calculations can then be expanded as-

$$H_{CCEI} = H_0^{A_c} + H_1^{A_c+1} + H_1^{A_c+2} + \dots \quad (6)$$

Here $H_0^{A_c}$, $H_0^{A_c+1}$, $H_0^{A_c+2}$ are called core, one body and two body cluster Hamiltonians respectively. This expansion is known as the valence cluster expansion. Similar to this Hamiltonian, any operator can be expanded in the valence space for the shell model calculations.

The two-body term is computed using Okubo-Lee-Suzuki (OLS) similarity transformation. We get a non Hermitian effective Hamiltonian in this procedure. The metric operator $S^\dagger S$ is used to make the Hamiltonian Hermitian. The resultant effective Hermitian Hamiltonian used for the shell model is $[S^\dagger S]^{1/2} H_{CCEI} [S^\dagger S]^{-1/2}$. Here, S is a matrix that diagonalizes H_{CCEI} .

Finally, we have also compared our *ab initio* results with shell model calculations using the phenomenological USDB interaction. The USDB interaction is fitted to two-body matrix elements [10], originally derived from a G-matrix approach. This interaction is fitted by varying 56 linear combinations of two-body matrix elements.

The shell model code NuShellX@MSU is a set of wrapper codes written by Alex Brown. It uses a proton-neutron basis. With this code, it is possible to diagonalize J-scheme matrix dimensions up to ~ 100 million.

III. RESULTS AND DISCUSSIONS

The experimental static and dynamic moments for Ne, Na, Mg and Al isotopes with up to 20 neutrons, at the borders of (or inside) the island of inversion, are reported in Refs. [14–28]. For explaining the intruder configuration of neutron rich nuclei ($\sim N = 20$), we need the $sd - pf$ model space. Using the SDPF-U-MIX effective interaction in the ref. [29], it is shown how the island of inversion region emerges around $N = 20$ and $N = 28$ for Ne to Al isotopes. The island of inversion is also known as island of deformation, which is due to nucleon-nucleon correlations. Because of the correlation energy we get a deform ground state band and the spherical mean field breaks. The normal order filling of orbits in the case of island of inversion candidates (^{30}Na , ^{31}Na , ^{31}Mg and ^{33}Al) vanishes, where ^{33}Al is found to be at the border of the island of inversion [28]. The IM-SRG and CCEI *ab initio* effective interactions contain excitations of particles within different shells (~ 13 oscillator major shells), and projected to a particular sd model space. The static and transitional quadrupole moments of nuclei lying in the island of inversion region show a drastic enhancement of quadrupole collectivity compared to neighboring nuclei. This has been attributed to a combination of a reduction in the $N = 20$ shell gap due to the tensor-part of the nucleon-nucleon monopole interaction and enhanced quadrupole correlations induced by neutron excitations across this reduced shell gap. The moments of these isotopes have been very well described using the phenomenological shell-model interactions in an enhanced $sd - pf$ model space where such neutron excitations are included, as illustrated e.g. in Refs. [20, 23, 28, 30]. The spectroscopy of other sd shell isotopes, including their moments, has been very well described by shell model calculations in the sd valence space using the phenomenological effective interactions, such as USDB [31]. However, the recent *ab initio* calculations reproduce also very well the spectroscopy of these sd shell isotopes, even improving towards an accurate description of their structure. It will be interesting to see how well they reproduce the ground state static and dynamic moments.

The magnetic dipole moment is defined as the expectation value of the dipole operator in the state with maximum M projection as

$$\mu = \langle J; M = J | \sum_i g_l(i) l_{z,i} + \sum_i g_s(i) s_{z,i} | J; M = J \rangle. \quad (7)$$

Here, g_l and g_s are the orbital and spin gyromagnetic ratios, respectively. Applying the Wigner-Eckart theorem

$$\mu = \frac{J}{(J(J+1)(2J+1))^{1/2}} \times$$

$$\langle J || \sum_i g_l(i) \mathbf{j}_i + (g_s(i) - g_l(i)) \mathbf{s}_i || \mathbf{J} \rangle. \quad (8)$$

The electric quadrupole moment operator is defined as

$$Q_z = \sum_{i=1}^A Q_z(i) = \sum_{i=1}^A e_i (3z_i^2 - r_i^2). \quad (9)$$

The spectroscopic quadrupole moment (Q_s) is defined as

$$Q_s(J) = \langle J, m = J | Q_2^0 | J, m = J \rangle \\ = \sqrt{\frac{J(2J-1)}{(2J+1)(2J+3)(J+1)}} \langle J || Q || J \rangle. \quad (10)$$

The calculated values of electromagnetic properties of sd shell nuclei with $e_p = 1.5e$, $e_n = 0.5e$; $g_s^{eff} = g_s^{free}$ using the two *ab initio* interactions as well as the phenomenological USDB shell model interaction in the sd model space, along with experimental data are shown in the Tables I-II. Magnetic moments have been taken from [32] and more recent data were obtained from a compilation maintained by T. Mertzimekis under the IAEA auspices [33]. Recently, the experimental quadrupole moments for sd shell nuclei have been evaluated and recommended values were presented in [34], along with shell model calculations using the USD and SDPF-U interactions. We used these experimental quadrupole moments in II. Values not available in this evaluation are taken from the specified reference.

For the oxygen isotopes, the calculated value of the magnetic moments with IM-SRG and CCEI show almost similar results. We have reported the magnetic moments for $^{17-20}\text{O}$ and quadrupole moments for $^{17-19}\text{O}$ isotopes. For ^{17}O the calculated magnetic moment and quadrupole moment values using all the interactions are similar, because this is the single-particle moment (similarly for ^{17}F). The calculated magnetic moment of the 4_1^+ state of ^{18}O and of the $5/2^+$ (g.s.) for ^{19}O and 2_1^+ state of ^{20}O is showing negative sign, while the sign has not yet been confirmed experimentally. In case of the quadrupole moment for ^{18}O , IMSRG and CCEI give opposite sign. USDB interaction supports CCEI result. The calculated value of magnetic moments for $^{17,18,19,20}\text{F}$ isotopes (g.s. and some isomers) are close to the experimental data. The results with IM-SRG for $\mu(5/2^+)$ for ^{21}F and $\mu(4^+)$ for ^{22}F are slightly lower in comparison with the experimental data, although the dominant wavefunction is the same for both interactions with nearly same probability. In case of quadrupole moments, experimental sign of $^{17-22}\text{F}$ isotopes are not yet confirmed. All the interactions give same sign except for ^{20}F .

The experimental data for magnetic moments of Ne isotopes are available from ^{19}Ne to ^{25}Ne , while

quadrupole moments are available for $^{21,22,23}\text{Ne}$. In Ref. [36] shell model results of magnetic moments are reported with USD and CW interactions for odd $^{23-25}\text{Ne}$ isotopes. Shape changes are reported to occur from collective to single particle in Ne isotopes when moving from ^{19}Ne to ^{25}Ne . It is shown that the magnetic moment is more sensitive than the quadrupole moment for deciding on the structure of the nucleus. Our calculated results using *ab initio* approaches for magnetic moments are showing good agreement. CCEI results are better in comparison to IM-SRG. We have reported the quadrupole moments for $^{20-23}\text{Ne}$ isotopes. Both *ab initio* results are in good agreement with the experimental data except for ^{20}Ne (the wavefunctions with CCEI and IM-SRG are given in Table III), USDB supports CCEI. For Ne isotopes overall CCEI results are in good agreement with the phenomenological and experimental data.

In the $^{26-31}\text{Na}$ chain [19], it is claimed that the experimental results of the magnetic moments for $^{26-29}\text{Na}$ are well described with sd model space using USD Hamiltonian. The disagreement appears for the $^{30-31}\text{Na}$ magnetic moments. The $^{30-31}\text{Na}$ isotopes are suggested to be members of the island of inversion, as shown by Utsuno et al. [37]. We have calculated the magnetic moments for the g.s. for $^{20-31}\text{Na}$ isotopes. In the case of $^{21,22}\text{Na}$ and ^{24}Na , the magnetic moments are also given for the first excited state. The results obtained from *ab initio* approaches for the g.s. are in reasonable agreement with the experimental values (Fig. 1). In general the CCEI results agree better than the IM-SRG. In the case of ^{24}Na , for the magnetic moment (for the first excited state), the sign is reverse using IM-SRG while CCEI gives the sign which is in agreement with the experimental data. We have calculated the quadrupole moments for $^{20-23}\text{Na}$ and $^{25-31}\text{Na}$. For ^{26}Na , *ab initio* effective interactions are giving opposite sign in comparison to the phenomenological effective interaction. Experimentally the sign has not yet been confirmed. In the case of ^{30}Na the results obtained from theory are far from the experimental value because ^{30}Na is an element of the island of inversion. To explain quadrupole moment for ^{30}Na we need pf model space. Utsuno et al. [47] performed theoretical calculations in $sd f_{7/2} p_{3/2}$ model space using SDPF-M interaction [48] for $^{27,29}\text{Na}$ isotopes using the Monte Carlo shell model approach.

For Mg isotopes, the sd shell model space is able to explain the experimental data reasonably good up to ^{29}Mg with CCEI and USDB. In case of ^{23}Mg , for the g.s. the experimental sign has not yet been confirmed for the both magnetic and quadrupole moments. Shell model predict negative sign for magnetic moment, while it is positive for quadrupole moment. In the case of ^{27}Mg , the negative magnetic moment for the ground state is dominated by $\nu s_{1/2}$ configuration. IM-SRG fails to reproduce the correct sign of its magnetic moment, although it is also predicting $\nu s_{1/2}$ configuration for the ground state. For ^{29}Mg , the g.s. spin is $I = 3/2$ ($\nu d_{3/2}$), all interactions are giving correct sign of the magnetic moment. The

sd model space is not able to reproduce correctly the measured ground state $1/2^+$ for ^{31}Mg . For this isotope a strongly prolate deformed ground state is reported in Ref. [16]. Recent theoretical results reveal the existence of 2p-2h and 4p-4h configurations for ^{32}Mg [49].

For $^{25-28,30-33}\text{Al}$ isotopes, the *sd* model space is able to correctly reproduce the magnetic moments. In most of the isotopes CCEI results are in good agreement with experimental data. For $^{25,28,30,32}\text{Al}$ isotopes, the sign for the g.s. magnetic moment is not yet confirmed, theoretically all interactions predict positive sign. The calculated $\mu(2^+)$ for ^{28}Al with IM-SRG and CCEI are not showing good agreement with experimental data. Experimentally, the sign of quadrupole moment is confirmed only for $^{26,27}\text{Al}$ isotopes. For both isotopes CCEI results agree with the experimental data.

In Si chain, the magnetic moments for $^{27,29,33}\text{Si}$ isotopes are calculated for the g.s. while for $^{28,30}\text{Si}$ isotopes for the first excited state. For $^{27-29}\text{Si}$ isotopes, the magnetic moments from CCEI approach are in good agreement. The quadrupole moment is calculated for ^{27}Si , ^{28}Si and ^{30}Si . For ^{30}Si , all the three interactions fail to reproduce the correct sign of the quadrupole moment.

We have also reported the magnetic moments of $^{28,29,31,32}\text{P}$, all the calculated results support positive sign for P isotopes in the g.s. except ^{32}P . For ^{32}P , IM-SRG supports the experimental sign but magnitude is far from the experimental value. We have calculated the magnetic moment of $^{31,32}\text{S}$ and quadrupole moment of $^{32,33}\text{S}$. The CCEI results for magnetic and quadrupole moments are in good agreement for $^{31,32,33}\text{S}$.

In the Fig. 1, we have shown the comparison between the experimental and theoretical magnetic dipole moments for F, Ne, Na, Mg, Al and P isotopes. The differences between the calculated and experimental data of the magnetic moments for Na isotopes above $A = 29$ are seen. The g.s. quadrupole moments for F, Na and Al isotopes are shown in the Fig. 2.

The occupancies of $d_{3/2}$, $d_{5/2}$ and $s_{1/2}$ proton and neutron orbitals for $^{19-22}\text{F}$, $^{19-23}\text{Ne}$, $^{20-31}\text{Na}$, $^{21-31}\text{Mg}$, $^{23,25-28,30-33}\text{Al}$, $^{27,29,33}\text{Si}$ and $^{28-29,31-32}\text{P}$ isotopes with CCEI for the g.s are shown in Fig. 3. In general the role of $d_{5/2}$ orbital is important as neutron number increases.

Discussions related to island of inversion candidates: for ^{30}Na (expt. g.s. is 2^+), IM-SRG and CCEI effective interactions predict g.s. as 0^+ , while USDB as 2^+ . The calculated magnetic and quadrupole moments

with USDB interaction is in good agreement with the experimental value in comparison to *ab initio* interactions. For ^{31}Na (expt. g.s. is $3/2^+$), CCEI predict correct g.s. while USDB and IM-SRG give $5/2^+$. The magnetic and quadrupole moments are very close to the experimental value using CCEI effective interaction. For ^{31}Mg (expt. g.s. is $1/2^+$), *ab initio* and USDB interactions give g.s. $3/2^+$. The calculated magnetic moment with CCEI is far from experimental value and also sign is not correct. For ^{33}Al , all the three interactions give g.s. as $5/2^+$, although experimentally it is not yet confirmed. We get good agreement with the experimental data for magnetic moment with CCEI and USDB interactions rather than IM-SRG. In the case of quadrupole moment sign is not yet confirmed experimentally, but magnitude is in good agreement with experimental value with CCEI and USDB interactions.

In Table III, we have shown the configuration of dominant wave functions for the nuclei using two *ab initio* interactions which give opposite sign of the quadrupole/magnetic moments.

IV. SUMMARY

In the present work using two *ab initio* approaches we have reported the quadrupole and magnetic moments for *sd* shell nuclei with the shell model. We perform calculations with effective interactions derived from in-medium similarity renormalization and coupled-cluster approaches. Along with *ab initio* interactions, we have also compared these results with the phenomenological USDB interaction. The results are showing good agreement with available experimental data. This work will add more information to previously known spectroscopic properties of *sd* shell nuclei from *ab initio* approaches.

Acknowledgment:

We would like to thank Prof. Gerda Neyens for many useful suggestions and comments on this manuscript. AS acknowledges financial support from MHRD (Govt. of India) for her Ph.D. thesis work. P.C.S. acknowledges financial support from faculty initiation grants.

-
- [1] T. Otsuka *et al.*, Phys. Rev. Lett. **105**, 032501 (2010).
 [2] J. D. Holt *et al.*, J. Phys. G **39**, 085111 (2012).
 [3] S.R. Stroberg *et al.*, Phys. Rev. C **93**, 051301(R) (2016).
 [4] G.R. Jansen *et al.*, Phys. Rev. C **94**, 011301(R) (2016).
 [5] G.R. Jansen *et al.*, Phys. Rev. Lett. **113**, 142502 (2014).
 [6] P.C. Srivastava and V. Kumar, Phys. Rev. C **94**, 064306 (2016).
 [7] E. Dikmen *et al.*, Phys. Rev. C **91**, 064301 (2015).
 [8] L. Caceres *et al.*, Phys. Rev. C **92**, 014327 (2015).
 [9] Zs. Vajta *et al.*, Phys. Rev. C **89**, 054323 (2014).
 [10] B. A. Brown and W. A. Richter, Phys. Rev. C **74**, 034315 (2006).
 [11] B. A. Brown and W. D. M. Rae, Nuclear Data Sheets **120**, 115 (2014).
 [12] S.K. Bogner, R.J. Furnstahl and A. Schwenk, Prog. Part. Nucl. Phys. **65**, 94 (2010).

TABLE I: Comparison of the experimental magnetic dipole moments (μ_N) with the theoretical values calculated using free g factors for sd shell nuclei. Experimental data are taken from Refs. [32, 35].

Nuclei	State	E_x (keV)	μ_{expt}	$\mu_{\text{IM-SRG}}$	μ_{CCEI}	μ_{USDB}
¹⁷ O	5/2 ⁺	0	-1.89379(9)	-1.913	-1.913	-1.913
¹⁸ O	2 ⁺	1982	-0.57(3)	-1.094	-1.022	-0.799
	4 ⁺	3555	2.5(4)	-2.455	-2.438	-2.172
¹⁹ O	5/2 ⁺	0	1.53195(7)	-1.509	-1.518	-1.531
	3/2 ⁺	96	-0.72(9)	-0.885	-0.869	-0.945
²⁰ O	2 ⁺	1674	0.70(3)	-0.921	-0.926	-0.716
¹⁷ F	5/2 ⁺	0	+4.7213(3)	+4.793	+4.793	+4.793
¹⁸ F	3 ⁺	937	+1.77(12)	+1.847	+1.826	+1.872
	5 ⁺	1121	+2.86(3)	+2.880	+2.880	+2.880
¹⁹ F	1/2 ⁺	0	+2.628868(8)	+2.917	+2.932	+2.898
	5/2 ⁺	197	3.595(13)	+3.560	+3.611	+3.584
²⁰ F	2 ⁺	0	+2.09335(9)	+2.171	+2.183	+2.092
²¹ F	5/2 ⁺	0	3.9194(12)	+2.868	+3.345	+3.779
²² F	4 ⁺	0	(+)2.6944(4)	+1.686	+2.477	+2.540
¹⁹ Ne	1/2 ⁺	0	-1.8846(8)	-2.060	-2.092	-2.037
	5/2 ⁺	238	-0.740(8)	-0.608	-0.669	-0.673
²⁰ Ne	2 ⁺	1634	+1.08(8)	+1.036	+1.037	+1.020
	4 ⁺	4247	+1.5(3)	+2.086	+2.095	+2.052
²¹ Ne	3/2 ⁺	0	-0.661797(5)	-0.656	-0.586	-0.750
	5/2 ⁺	351	0.49(4)	+0.023	-0.365	-0.574
²² Ne	2 ⁺	1275	+0.65(2)	+1.108	+0.550	+0.748
	4 ⁺	3357	+2.2(6)	+2.800	+1.332	+2.044
²³ Ne	5/2 ⁺	0	-1.077(4)	-0.965	-0.786	-1.050
²⁵ Ne	1/2 ⁺	0	-1.0062(5)	-0.710	-0.924	-0.928
²⁰ Na	2 ⁺	0	+0.3694(2)	+0.390	+0.330	+0.446
²¹ Na	3/2 ⁺	0	+2.83630(10)	+1.533	+2.388	+2.489
	5/2 ⁺	332	3.7(3)	+3.228	+3.196	+3.355
²² Na	3 ⁺	0	+1.746(3)	+0.524	+1.806	+1.791
	1 ⁺	583	+0.523(11)	+0.989	+0.529	+0.518
²³ Na	3/2 ⁺	0	+2.2176556(6)	+1.414	+1.887	+2.098
²⁴ Na	4 ⁺	0	+1.6903(8)	+0.890	+1.285	+1.631
	1 ⁺	472	-1.931(3)	+0.764	-0.881	-1.865
²⁵ Na	5/2 ⁺	0	+3.683(4)	+4.301	+3.361	+3.367
²⁶ Na	3 ⁺	0	+2.851(2)	+3.536	+2.360	+2.632
²⁷ Na	5/2 ⁺	0	+3.895(5)	+4.041	+3.623	+3.647
²⁸ Na	1 ⁺	0	+2.426(5)	+2.392	+1.760	+2.081
²⁹ Na	3/2 ⁺	0	+2.449(8)	+2.548	+2.198	+2.438
³⁰ Na	2 ⁺	0	+2.083(10)	+3.363	+2.883	+2.418
³¹ Na	3/2 ⁺	0	+2.305(8)	+3.015	+2.551	+2.614
²¹ Mg	5/2 ⁺	0	-0.983(7)	-0.259	-0.351	-0.848
²³ Mg	3/2 ⁺	0	0.5364(3)	-0.112	-0.218	-0.410
²⁴ Mg	2 ⁺	1369	+1.076(26)	+1.919	+1.094	+1.026
	4 ⁺	4123	+1.6(12)	+3.546	+2.169	+2.070
	2 ⁺	4238	+1.2(4)	+1.852	+1.062	+1.037
	4 ⁺	6010	+2.0(16)	+3.850	+2.115	+2.048
²⁵ Mg	5/2 ⁺	0	-0.85545(8)	-0.460	-0.197	-0.849
²⁶ Mg	2 ⁺	1809	+1.0(3)	+1.904	+1.281	+1.739
²⁷ Mg	1/2 ⁺	0	-0.411(2)	+0.321	-0.256	-0.412

TABLE I: Continuation.

Nuclei	State	E_x (keV)	μ_{expt}	μ_{IM-SRG}	μ_{CCEI}	μ_{USDB}
^{29}Mg	$3/2^+$	0	+0.9780(6)	+1.735	+1.470	+1.071
^{31}Mg	$1/2^+$	0	-0.88355(15)	-0.563	+1.406	-0.923
^{23}Al	$5/2^+$	0	+3.889(5)	+4.682	+3.681	+3.866
^{24}Al	1^+	426	2.99(9)	-1.537	+2.071	+2.985
^{25}Al	$5/2^+$	0	3.6455(12)	+3.986	+3.142	+3.655
^{26}Al	5^+	0	+2.804(4)	+3.375	+2.907	+2.839
^{27}Al	$5/2^+$	0	+3.6415069(7)	+4.336	+2.461	+3.455
^{28}Al	3^+	0	3.242(5)	+4.245	+2.378	+3.098
	2^+	31	+4.3(4)	+0.870	+0.675	+3.215
^{30}Al	3^+	0	3.010(7)	+3.742	+3.455	+3.039
^{31}Al	$(5/2^+)$	0	+3.830(5)	+5.127	+3.863	+3.761
^{32}Al	1^+	0	1.952(2)	+2.502	+1.811	+1.612
^{33}Al	$(5/2^+)$	0	+4.088(5)	+5.681	+4.268	+4.224
^{27}Si	$5/2^+$	0	(-)0.8554(4)	+0.251	+0.337	-0.678
^{28}Si	2^+	1779	+1.1(2)	+1.495	+1.093	+1.031
^{29}Si	$1/2^+$	0	-0.55529(3)	-0.083	-0.575	-0.503
^{30}Si	2^+	2235	+0.8(2)	+1.226	+1.939	+0.732
^{33}Si	$(3/2^+)$	0	1.21(3)	+1.844	+1.803	+1.206
^{28}P	3^+	0	0.312(3)	+3.041	+1.076	+0.302
^{29}P	$1/2^+$	0	1.2346(3)	+3.174	+1.348	+1.133
^{31}P	$1/2^+$	0	+1.13160(3)	+2.422	+1.694	+1.087
	$3/2^+$	1270	+0.30(8)	-0.384	-0.063	+0.167
	$5/2^+$	2230	+2.8(5)	+2.190	+3.097	+2.218
^{32}P	1^+	0	-0.2524(3)	-1.105	+0.177	-0.021
^{31}S	$1/2^+$	0	0.48793(8)	+0.415	-1.003	-0.441
^{32}S	2^+	2231	+0.9(2)	+1.377	+0.980	+1.010
	4^+	4459	+1.6(6)	+2.998	+1.840	+2.028

- [13] K. Tsukiyama, S.K. Bogner and A. Schwenk, Phys. Rev. Lett. **106**, 222502 (2011).
- [14] H. Iwasaki *et al.*, Phys. Lett. B **620**, 118 (2005).
- [15] B. V. Pritychenko *et al.*, Phys. Lett. B **461**, 322 (1999).
- [16] G. Neyens *et al.*, Phys. Rev. Lett. **94**, 022501 (2005).
- [17] M. D. Rydt *et al.*, Phys. Lett. B **678**, 344 (2009).
- [18] P. Himpe *et al.*, Phys. Lett. B **643**, 257 (2006).
- [19] M. Keim *et al.*, Eur. Phys. J. A **8**, 31 (2000).
- [20] P. Doornenbal *et al.*, Phys. Rev. C **93**, 044306 (2016).
- [21] A.M. Hurst *et al.*, Phys. Lett. B **674**, 168 (2009).
- [22] M. Seidlitz *et al.*, Phys. Rev. C **89**, 024309 (2014).
- [23] O. Niedermaier *et al.*, Phys. Rev. Lett. **94**, 172501 (2005).
- [24] M. Seidlitz *et al.*, Phys. Lett. B **700**, 181 (2011).
- [25] J. A. Church *et al.*, Phys. Rev. C **72**, 054320 (2005).
- [26] D. Borremans *et al.*, Phys. Lett. B **537**, 45 (2002).
- [27] D. Kameda *et al.*, Phys. Lett. B **647**, 93 (2007).
- [28] H. Heylen *et al.*, Phys. Rev. C **94**, 034312 (2016).
- [29] E. Caurier, F. Nowacki and A. Poves, Phys. Rev. C **90**, 014302 (2014).
- [30] Y. Utsuno, T. Otsuka, T. Glasmacher, T. Mizusaki, and M. Honma, Phys. Rev. C **70**, 044307 (2004).
- [31] W. A. Richter, S. Mkhize, and B. Alex Brown, Phys. Rev. C **78**, 064302 (2008).
- [32] N. J. Stone, Atomic Data and Nuclear Data Tables **90**, 75 (2005).
- [33] IAEA <https://www-nds.iaea.org/nuclearmoments/>.
- [34] M. De Rydt, M. Depuydt and G. Neyens, Atomic Data and Nuclear Data Tables **99**, 391 (2013).
- [35] Data extracted using the NNDC World Wide Web site from the ENSDF database.
- [36] W. Geithner *et al.*, Phys. Rev. C **71**, 064319 (2005).
- [37] Y. Utsuno *et al.*, Phys. Rev. C **64**, 011301(R) (2001).
- [38] N. J. Stone, Atomic Data and Nuclear Data Tables **111-112**, 1 (2016).
- [39] G. Neyens *et al.*, Eur. Phys. J. Special Topics **150**, 149 (2007).
- [40] A. Halkier *et al.*, Chemical Physical Letters **271**, 273 (1997).
- [41] D. Sundholm and J. Olsen, Journal of Physical Chemistry **96**, 627 (1992).
- [42] P. Pyykkö, Chemical Physical Letters **227**, 221 (1994).
- [43] D. Sundholm and J. Olsen, Nucl. Phys. A **534**, 360 (1991).
- [44] V. Kellö *et al.*, Chemical Physical Letters **304**, 414 (1999).
- [45] K. Matsuta *et al.*, Nucl. Phys. A **704**, 98c (2002).
- [46] D. Sundholm and J. Olsen, Phys. Rev. A **42**, 1160 (1990).
- [47] Y. Utsuno *et al.*, Phys. Rev. C **70**, 044307 (2004).

TABLE II: Comparison of the experimental quadrupole moments (eb) with the theoretical values calculated by using $e_p=1.5e$ and $e_n=0.5e$.

Nuclei	State	E_x (keV)	Q_{expt}	$Q_{\text{IM-SRG}}$	Q_{CCEI}	Q_{USDB}	Ref.
^{17}O	$5/2^+$	0	-0.02558(22)	-0.0302	-0.0302	-0.0302	[41]
^{18}O	2^+	1982	-0.036(9)	+0.0300	-0.0172	-0.0294	[38]
^{19}O	$5/2^+$	0	0.00362(13)	-0.0079	+0.0005	-0.0026	[34]
^{17}F	$5/2^+$	0	0.0799(34)	-0.0907	-0.0907	-0.0907	[34]
^{18}F	5^+	1121	0.077(5)	-0.1226	-0.1226	-0.1224	[38]
^{19}F	$5/2^+$	197	0.0942(9)	-0.0204	-0.01056	-0.1045	[40]
^{20}F	2^+	0	0.0547(18)	-0.0515	+0.0729	+0.0679	[34]
^{21}F	$5/2^+$	0	0.0943(33)	-0.0734	-0.1175	-0.1199	[34]
^{22}F	4^+	0	0.003(2)	-0.0228	-0.0249	-0.0078	[38]
^{20}Ne	2^+	1634	-0.23(3)	+0.0359	-0.1578	-0.1576	[38]
^{21}Ne	$3/2^+$	0	+0.10155(75)	+0.0441	+0.1109	+0.1119	[34, 41]
^{22}Ne	2^+	1257	-0.19(4)	-0.0728	-0.1536	-0.1532	[38]
^{23}Ne	$5/2^+$	0	+0.1429(43)	+0.0939	+0.1699	+0.1629	[34]
^{20}Na	2^+	0	0.1009(88)	-0.0344	+0.100	+0.0946	[34]
^{21}Na	$3/2^+$	0	0.137(12)	+0.0469	+0.1216	+0.1218	[34]
^{22}Na	3^+	0	+0.167(17)	+0.0953	+0.2405	+0.2506	[34]
^{23}Na	$3/2^+$	0	+0.104(1)	+0.0546	+0.1246	+0.1180	[34, 42]
^{25}Na	$5/2^+$	0	0.00146(22)	+0.0257	+0.0674	+0.0025	[34]
^{26}Na	3^+	0	0.00521(20)	+0.0219	+0.0239	-0.0051	[34]
^{27}Na	$5/2^+$	0	0.00708(24)	+0.0214	-0.0035	-0.0127	[34]
^{28}Na	1^+	0	0.0389(11)	+0.0326	+0.0368	+0.0495	[34]
^{29}Na	$3/2^+$	0	+0.0842(25)	+0.0746	+0.1046	+0.0791	[34]
^{30}Na	2^+	0	+0.146(1.6)	-0.0743	-0.1048	-0.1149	[39]
^{31}Na	$3/2^+$	0	+0.105(2.5)	+0.0471	+0.0920	+0.0583	[39]
^{23}Mg	$3/2^+$	0	0.1133(37)	+0.0331	+0.1322	+0.1229	[34]
^{24}Mg	2^+	1369	-0.29(3)	-0.058	-0.1857	-0.1931	[38]
^{25}Mg	$5/2^+$	0	+0.1994(20)	+0.0747	+0.1809	+0.2243	[43]
^{26}Mg	2^+	1809	-0.21(2)	-0.0632	+0.1155	-0.1439	[38]
^{25}Al	$5/2^+$	0	0.249(18)	+0.0374	+0.1813	+0.2018	[34]
^{26}Al	5^+	0	+0.259(29)	+0.072	+0.294	+0.3028	[34]
^{27}Al	$5/2^+$	0	+0.1466(10)	+0.032	+0.091	+0.1803	[34, 44]
^{28}Al	3^+	0	0.172(12)	+0.0604	+0.1388	+0.1877	[34]
^{31}Al	$5/2^+$	0	0.1365(23)	+0.0826	+0.1320	+0.1706	[28]
^{32}Al	1^+	0	0.0250(21)	+0.0210	+0.006	+0.0310	[34]
^{33}Al	$5/2^+$	0	0.141(3)	+0.1003	+0.1368	+0.1390	[28]
^{27}Si	$5/2^+$	0	0.063(14)	+0.0205	+0.072	+0.1409	[45]
^{28}Si	2^+	1779	+0.16(3)	+0.0704	+0.196	+0.2087	[38]
^{30}Si	2^+	2235	-0.05(6)	+0.0292	+0.1470	+0.0239	[38]
^{32}S	2^+	1941	-0.15(2)	+0.0133	-0.0801	-0.1283	[38]
^{33}S	$3/2^+$	0	-0.0678(13)	-0.0230	-0.0565	-0.0736	[46]

[48] Y. Utsuno *et al.*, Phys. Rev. C **60**, 054315 (1999).

(2016).

[49] A.O. Macchiavelli *et al.*, Phys. Rev. C **94**, 051303(R)

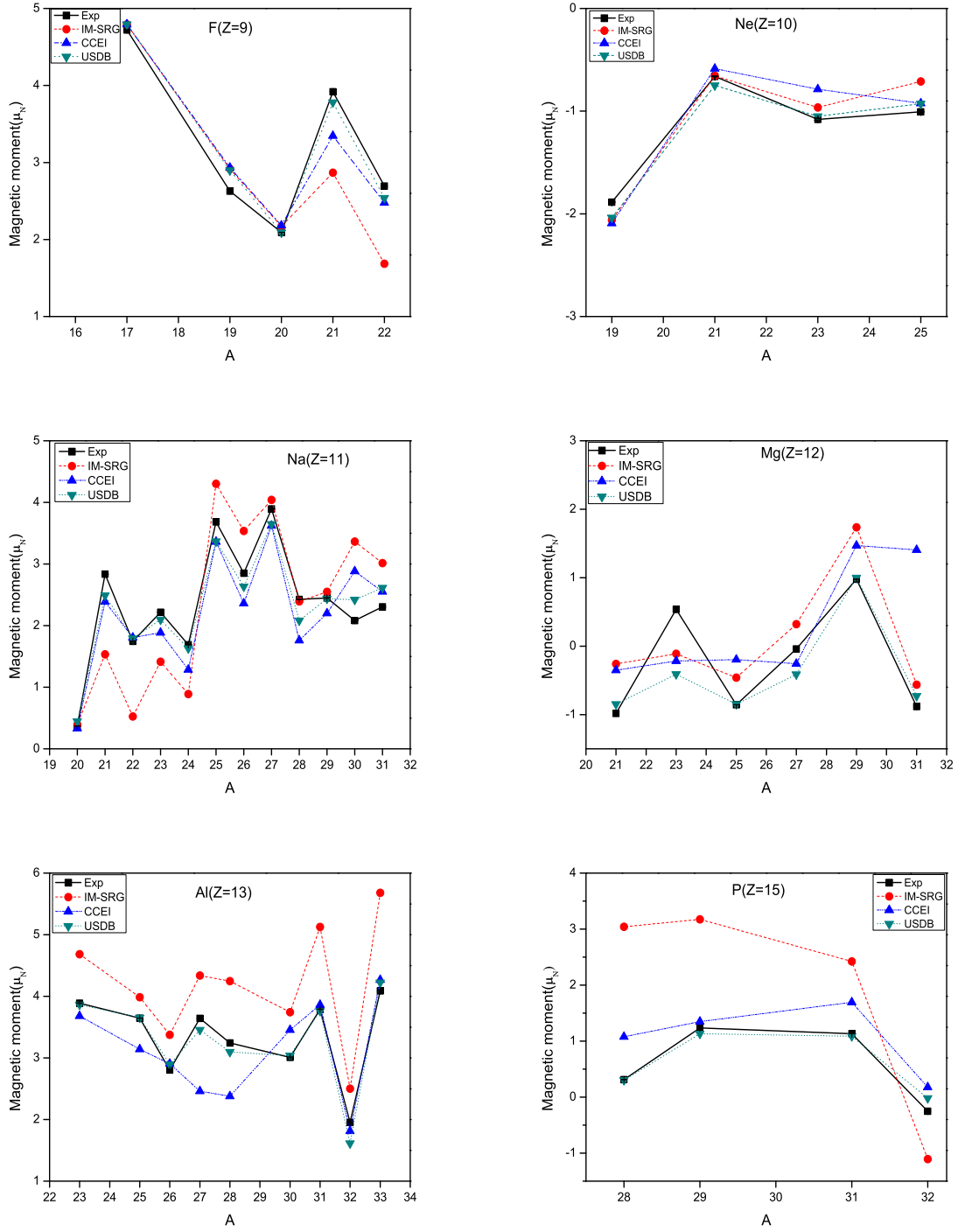


FIG. 1: Comparison between the experimental and theoretical magnetic dipole moments for F, Ne, Na, Mg, Al and P isotopes. The calculated shell model signs are used in the case when it was not measured.

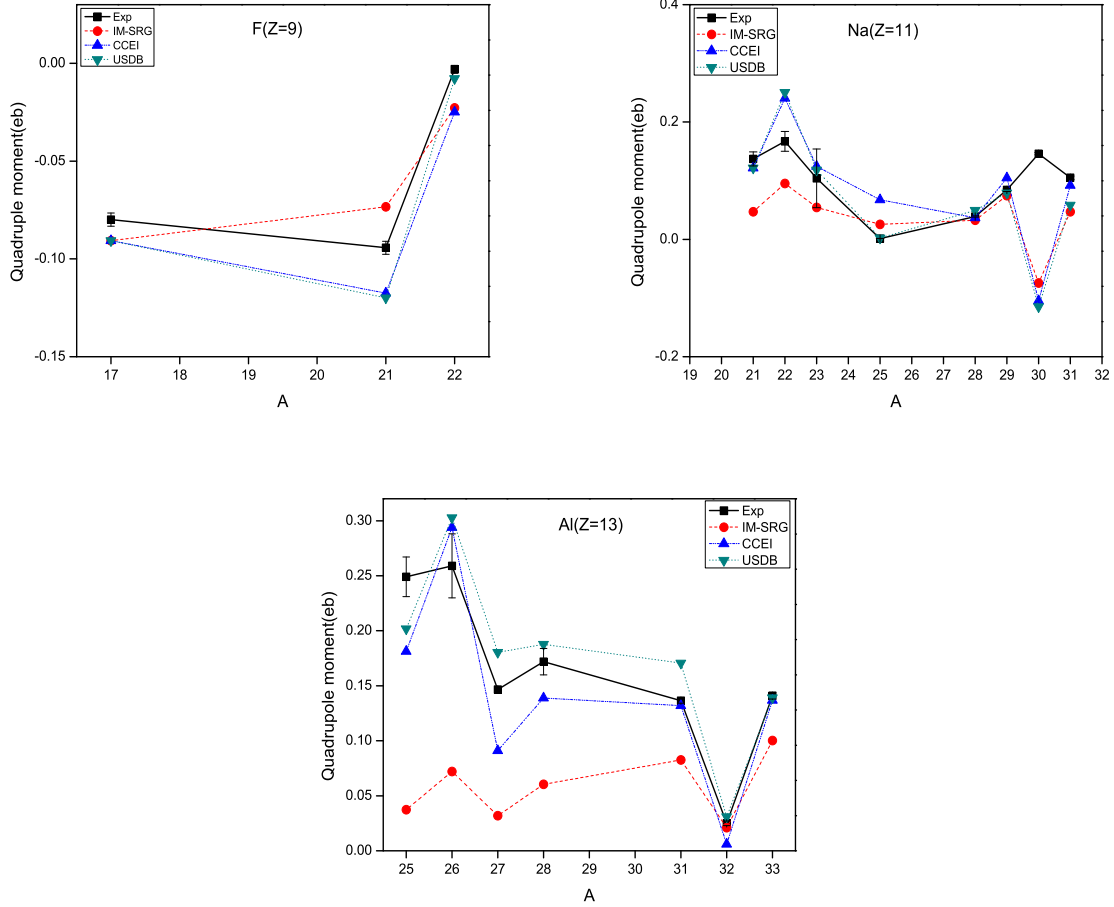


FIG. 2: Comparison between experimental and theoretical quadrupole moments for F, Na and Al isotopes. The calculated shell model signs are used in case when it was not measured.

TABLE III: Dominant configuration of the wave functions with CCEI and IM-SRG which predict opposite sign of the quadrupole/magnetic moments for ^{18}O , ^{20}Ne , ^{24}Na , $^{26,27,31}\text{Mg}$, ^{32}P and ^{32}S .

Nuclei	Moment	CCEI	Probability	IM-SRG	Probability
^{18}O	Q_{2^+}	$\pi(d_{3/2}^0, d_{5/2}^0, s_{1/2}^0) \otimes \nu(d_{3/2}^0, d_{5/2}^2, s_{1/2}^0)$	77.74%	$\pi(d_{3/2}^0, d_{5/2}^0, s_{1/2}^0) \otimes \nu(d_{3/2}^0, d_{5/2}^2, s_{1/2}^0)$	79.69%
^{20}Ne	Q_{2^+}	$\pi(d_{3/2}^0, d_{5/2}^2, s_{1/2}^0) \otimes \nu(d_{3/2}^0, d_{5/2}^2, s_{1/2}^0)$	18.41%	$\pi(d_{3/2}^0, d_{5/2}^2, s_{1/2}^0) \otimes \nu(d_{3/2}^0, d_{5/2}^2, s_{1/2}^0)$	18.26%
^{24}Na	μ_{1^+}	$\pi(d_{3/2}^0, d_{5/2}^3, s_{1/2}^0) \otimes \nu(d_{3/2}^0, d_{5/2}^5, s_{1/2}^0)$	14.47%	$\pi(d_{3/2}^0, d_{5/2}^3, s_{1/2}^0) \otimes \nu(d_{3/2}^0, d_{5/2}^4, s_{1/2}^1)$	15.75%
^{26}Mg	Q_{2^+}	$\pi(d_{3/2}^0, d_{5/2}^3, s_{1/2}^1) \otimes \nu(d_{3/2}^0, d_{5/2}^4, s_{1/2}^2)$	7.89%	$\pi(d_{3/2}^0, d_{5/2}^3, s_{1/2}^1) \otimes \nu(d_{3/2}^1, d_{5/2}^4, s_{1/2}^1)$	8.04%
^{27}Mg	$\mu_{1/2^+}$	$\pi(d_{3/2}^0, d_{5/2}^4, s_{1/2}^0) \otimes \nu(d_{3/2}^0, d_{5/2}^6, s_{1/2}^1)$	30.27%	$\pi(d_{3/2}^0, d_{5/2}^4, s_{1/2}^0) \otimes \nu(d_{3/2}^0, d_{5/2}^6, s_{1/2}^1)$	24.16%
^{31}Mg	$\mu_{1/2^+}$	$\pi(d_{3/2}^0, d_{5/2}^3, s_{1/2}^1) \otimes \nu(d_{3/2}^3, d_{5/2}^6, s_{1/2}^2)$	51.23%	$\pi(d_{3/2}^0, d_{5/2}^4, s_{1/2}^0) \otimes \nu(d_{3/2}^4, d_{5/2}^6, s_{1/2}^1)$	77.40%
^{32}P	μ_{1^+}	$\pi(d_{3/2}^0, d_{5/2}^6, s_{1/2}^1) \otimes \nu(d_{3/2}^1, d_{5/2}^6, s_{1/2}^2)$	64.52%	$\pi(d_{3/2}^1, d_{5/2}^6, s_{1/2}^0) \otimes \nu(d_{3/2}^2, d_{5/2}^6, s_{1/2}^1)$	9.47%
^{32}S	Q_{2^+}	$\pi(d_{3/2}^0, d_{5/2}^6, s_{1/2}^2) \otimes \nu(d_{3/2}^1, d_{5/2}^6, s_{1/2}^1)$	36.14%	$\pi(d_{3/2}^1, d_{5/2}^6, s_{1/2}^1) \otimes \nu(d_{3/2}^2, d_{5/2}^6, s_{1/2}^0)$	3.69%

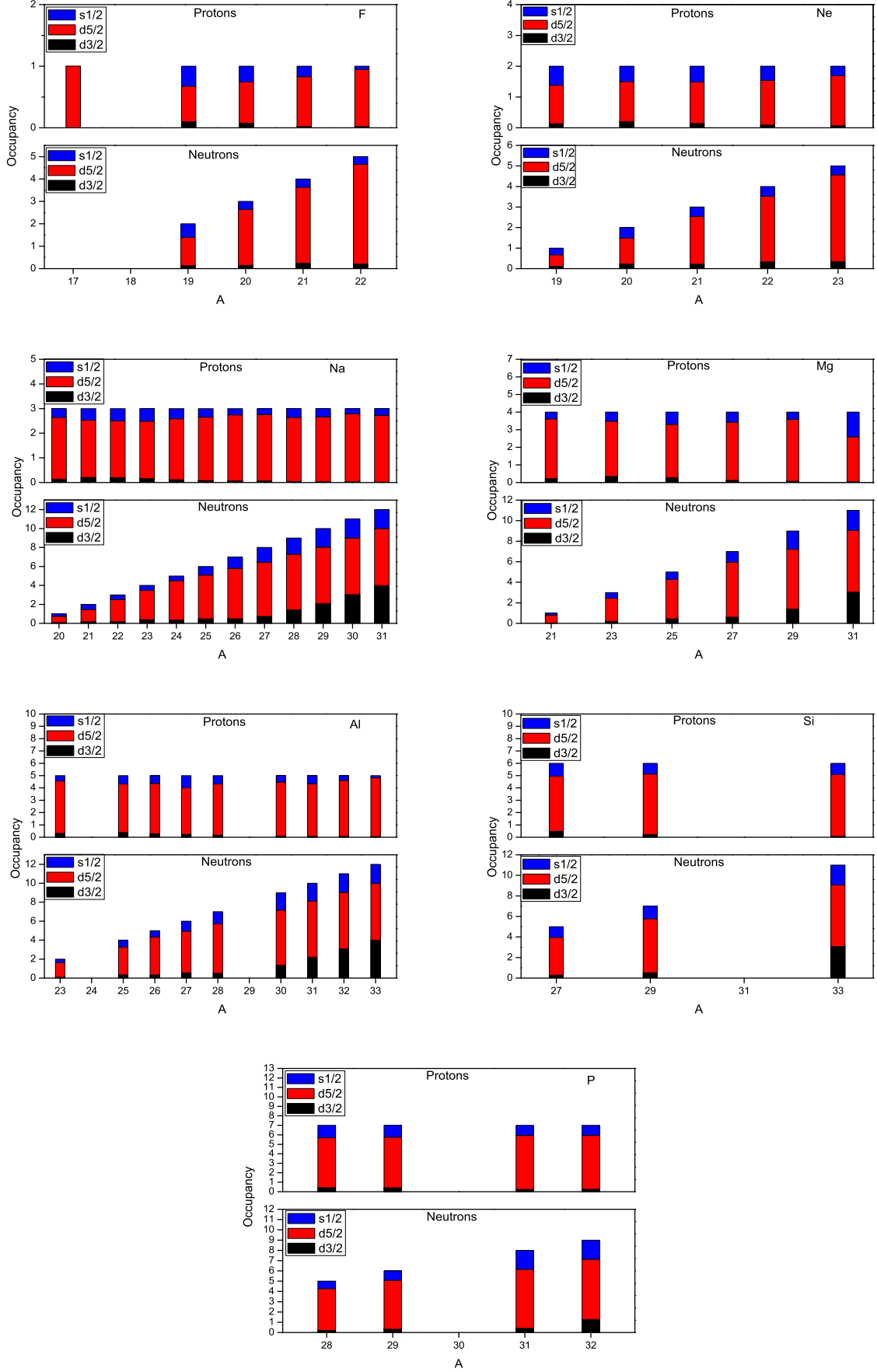


FIG. 3: Occupancies of $d_{3/2}$, $d_{5/2}$ and $s_{1/2}$ proton and neutron orbitals for $^{19-22}\text{F}$, $^{19-23}\text{Ne}$, $^{20-31}\text{Na}$, $^{21-31}\text{Mg}$, $^{23,25-28,30-33}\text{Al}$, $^{27,29,33}\text{Si}$ and $^{28-29,31-32}\text{P}$ isotopes with CCEI for the g.s. We have reported occupancies of those nuclei for which the quadrupole/magnetic moments are calculated in the present work.